A Teaching Tool for Phasor Measurement Estimation

Daniel Dotta, *Member, IEEE*, Joe H. Chow, *Fellow, IEEE* and David B. Bertagnolli *Senior Member, IEEE*

***Abstract*—This paper discusses the design and usage of a SIMULINK-based Phasor Measurement Unit (PMU) simulator package [1]. The motivation for developing the package is to provide a flexible environment for teaching phasor measurement and frequency estimation to advanced undergraduate and graduate students, and a knowledge base for research and development. This software allows for the exploration of the algorithms and phenomena involved in the phasor estimation process. The package is built on the SIMULINK platform and is able to process simulated signals as well as measured point-on-wave data.**

***Index Terms*—PMU, phasor data processing, power system analysis, phasor estimation algorithms.**

I. INTRODUCTION

THe use of Phasor Measurement Unit (PMU) data in power system operation is of increasing interest. Power grid operators have started to recognize the potential of this technology and several Wide Area Measurement Systems (WAMS) are being built around the world [1–3]. The number of PMUs installed and connected to WAMS in large power systems, such as in the USA and China, is already over several thousands [3, 4]. In recent years, many real-time and off-line application tools have been developed using phasor measurement data. In particular, PMU data are used extensively for postmortem analysis [5]. Some examples can be found in recent Brazilian [6] and Colombian [7] blackouts.

Despite the high level of research activities in the development of PMU applications [8], the dissemination of phasor processing techniques within a PMU is quite limited. In addition to being a high-sampling-rate digital recording device with GPS-signal time-tagging, a PMU uses signal processing techniques to provide frequency and phasor information on voltages and currents. The signal processing part is not specified in the IEEE C37.118 Synchrophasor Standard [9]. As a result, there are various implementations with different algorithms and data windows. A good understanding of the tradeoff between various algorithms would be useful to power engineering students who may get involved in the design of the next-generation of power system measurement equipment. This will also help operation and maintenance engineers to recognize and report PMU data issues.

This paper reports on a software tool based on the SIMULINK platform that can be used for teaching and research to explore the algorithms involved in the phasor measurement process. The main goal is to replicate the device architecture and conventional algorithms available in the literature. This SIMULINK software platform is an evolution of the MATLAB software platform presented in [10]. The SIMULINK software platform shows clearly the various functional blocks with in a real PMU, and can be readily used for simulation and symmetrical component analysis. The relevant parameters such as the input sine wave amplitude, frequency, and phase, can be changed on-the-fly. This software tool will provide hands-on experience for understanding the algorithms and tradeoffs involved in the phasor measurement process, such as off-nominal frequency and unbalanced phase operation, and impact of correction factors for off-nominal frequency signal.

The paper is organized as follows. In Section II, the basic architecture of a phasor measurement device is described. In Section III, a SIMULINK-based PMU simulator is presented. In Section IV, the education activities of the proposed approach are presented. Conclusions are presented in Section V.

II. BASIC PHASOR MEASUREMENT ARCHITECTURE

Figure 1 shown a general block diagram of a PMU [11]. The proposed PMU simulator is shown in Figure 2, with three main computing blocks

- Phasor estimation using *Discrete Fourier Transform* (DFT)
- Frequency estimation
- Post-processing including calibration factors and filtering

Not included in the PMU simulator are the input signal anti-aliasing filter, the GPS-based timing signal generator, and the A/D converter for sampling the filtered input signal.

The purpose of the PMU simulator is to explore the phasor and frequency estimation, and the techniques involved in correcting the phasor estimation under off-nominal frequency

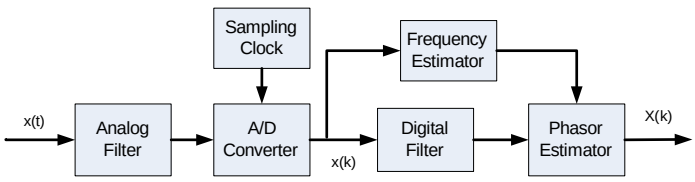

Fig. 1. PMU General Blocks

Daniel Dotta is with the Federal Institute of Santa Catarina, Florianópolis, SC 88020-300, Brazil. (email:dotta@ifsc.edu.br).

J.H. Chow is with Rensselaer Polytechnic Institute, Troy, NY 12180, USA. (email:chowj@rpi.edu).

D. Bertagnolli is with ISO-NE, Holyoke, MA 01040, USA. (e-mail: dbertagnolli@iso-ne.com).

[1]The simulator and PMU data is avaible upon request from the first author.

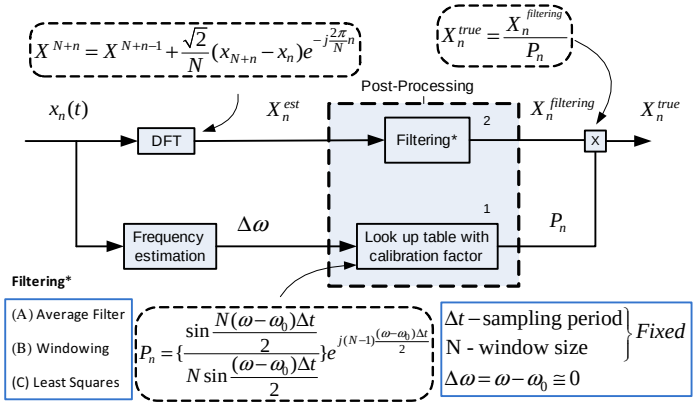

Fig. 2. Phasor processing algorithm for uniform sampling [5]

operation. To simplify the proposed simulator, two assumptions are made:

- the sampling rate is uniform
- anti-aliasing filtering has been applied to the input signals

Note that non-uniform sampling schemes based on the estimated system frequency have been proposed [12, 13]. The technicalities of these schemes are quite advanced and the implementations of such schemes can be quite difficult.

A. Phasor Estimation

The function of this phasor estimation block is to compute the amplitude and phase of an input signal at the fundamental frequency using DFT. The non-recursive DFT algorithm is given by

$$X^k = \frac{\sqrt{2}}{N}\sum_{n=0}^{N-1} x_{k+n}e^{-j\frac{2\pi n}{N}} \tag{1}$$

where k is the first sample in the data window, and N is the number of samples in a cycle of the fundamental frequency component. If a recursive DFT approach is used, care must be taken so that the algorithm does not accumulate truncation errors during long-term operation.

B. Frequency Estimation

In normal power system operation, the power system frequency seldom stays exactly at the nominal system frequency (50 or 60 Hz). The frequency measurement is important because the phasor is a steady-state representation so correction must be done in the presence of frequency deviations. This deviation can be small, when subject to random load variation, or large, during loss of generation disturbances. Thus, the frequency estimation methodology plays a key role in the phasor computation process. An interesting discussion of the power system frequency concept is found in [11].

Frequency measurement on a power system is not an instantaneous measured value, like that obtained from a machine speed sensor installed on the shaft of a generator. Instead, frequency is calculated from a voltage waveform data window. Several frequency measurement methodologies can be found in the literature [14–18]. The phasor-based method [15, 17, 18] is chosen as the frequency estimator for the PMU Simulator. This method, commonly used in commercial PMUs, is a by-product of the phasor estimation and provides satisfactory performance under large frequency variation and noisy environment. This method, originally proposed in [19], defines frequency as the speed of rotation of a phasor. The main idea is to calculate the positive-sequence voltage phasor for a balanced system operating at off-nominal frequency, while still using the nominal frequency-based DFT and samples. The method proposed in [19] is based on a fixed-frequency model. The method implemented in the PMU Simulator here is described in [17], which considers the effect of dynamic frequency in the algorithm.

In [17], the authors mathematically prove that frequency can be accurately measured using sample phasor measurement series, shown in Figure 3, where (A,B) and (D,E) are phasor measurement samples, N is the size of the data window for phasor calculation, and M is the size of the data window for frequency calculation. The frequency deviation is computed as

$$\Delta\omega = \frac{\varphi^{D-E} - \varphi^{A-B}}{M\Delta t} \tag{2}$$

C. Post-Processing

Under off-nominal frequency operation, the post-processing block is necessary to correct for the effects caused by the leakage phenomenon, resulting from the truncation of sampled data outside the data window. Consequently, the estimated phasor (X^{est}) is attenuated by two complex gains, P_n and Q_n such as,

$$X^{est} = P_n X^{true} + Q_n X^{true} \tag{3}$$

where

$$P_n = \left\{\frac{\sin\frac{N(\omega-\omega_0)\Delta t}{2}}{N\sin\frac{(\omega-\omega_0)\Delta t}{2}}\right\}e^{j(N-1)\frac{(\omega-\omega_0)\Delta t}{2}} \tag{4}$$

$$Q_n = \left\{\frac{\sin\frac{N(\omega+\omega_0)\Delta t}{2}}{N\sin\frac{(\omega+\omega_0)\Delta t}{2}}\right\}e^{-j(N-1)\frac{(\omega+\omega_0)\Delta t}{2}} \tag{5}$$

From Equation (4), the effects of the complex gain P_n (shown in Figure 2) can be readily computed from the sampling window size (N), the frequency deviation ($\Delta\omega$), and the sampling period ($\triangle t$) [20]. The magnitude of P_n is an attenuation factor, and the phase angle of P_n is a constant offset in the measured phase angles. As the window size (N) and sampling period ($\triangle t$) are fixed, P_n can be readily estimated for a frequency range and stored in a table (Block 1 in Figure 2). In real-time, frequency deviation estimation is necessary to compute the correct P_n value. The complex gains Q_n introduces a variation at frequency $2\omega_0 + \Delta\omega \simeq 2\omega_0$ in

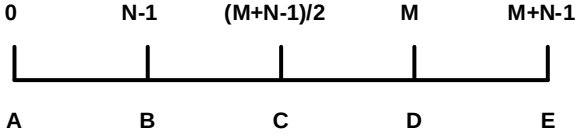

Fig. 3. Phasor-Based Frequency Estimation [17]

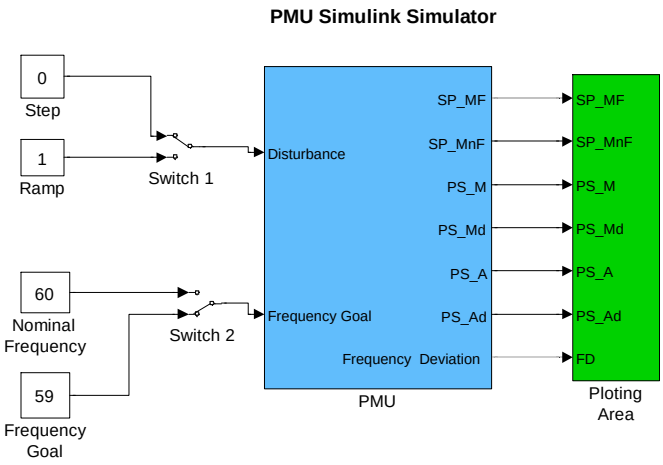

Fig. 4. Main Window

the estimated single-phase phasor. In contrast to a static offset, this oscillation is not readily removed. A conventional way to minimize its influence is to use a three-point-average filter [20]. Other filtering techniques are described in [21].

III. SIMULINK-BASED PMU SIMULATOR

A SIMULINK PMU simulator suitable for exploring the phasor measurement estimation process is shown in Figure 4. The simulator works with single-phase and three-phase measurement signals, allowing positive-sequence phasor estimation. Step and ramp (frequency modulation) frequency disturbances can be simulated to observe the influence of the complex gains (P_n and Q_n) and filtering in the phasor estimation process. Processing of real point-on-wave data can also be realized.

The main features of the PMU Simulator are:

- Non-Recursive DFT
- Off-nominal frequency operation
- Unbalanced input signals
- Symmetrical components estimation
- P_n and Q_n complex gains effects
- On-the-fly frequency changes.

The main goal of the simulator is to show the PMU performance under off-nominal frequency operation. It is important to understand how a steady-state phasor concept can be applied under off-nominal frequency environment. Two frequency disturbances are considered and can be chosen using *Switch 1* in Figure 4: step and ramp. The level of the disturbance can also be selected in the main window using *Switch 2* in Figure 4. The frequency level can also be changed on-the-fly. A variety of signals are available for plotting: single-phase and positive-sequence magnitude and angle with and without filtering, and down-sampled positive-sequence magnitude and phase. To understand the internal PMU operation a user can click on the main block to gain access to the internal SIMULINK blocks.

The software blocks and algorithms involved in the SIMULINK PMU simulator are shown in Figure 5 and are described as follows.

A. Three-Phase Sinusoidal Wave Generation (Figure 19)

- Inputs: disturbances type and frequency disturbance level
- Function: In this block the sinusoidal waves in three-phase power systems are generated and the disturbance types are processed. The three-phase signal magnitude and phase can be changed allowing unbalanced operation. A bias factor can also be set to introduce off-set and noise in the sinusoid waves. Real data files can also be used.
- Outputs: Three-phase (A, B, C) digital sinusoid waves

B. Phasor Estimation (Figure 6)

- Inputs: Three-phase (A, B, C) digital sinusoid waves or measured point-on-wave data
- Function: The function consists of three single-phase estimation, using a data buffer of window size (N). This data frame is sent to the *FFT* block. The non-recursive DFT algorithm described in Section II-A is used . The estimation using rectangular coordinates is computed for each new data window. The FFT block output consists of N harmonic frequency spectral values. In the phasor estimation process only the fundamental component is used so an extra block is used to extract the first harmonic. The *Gain* block represents the constant $\sqrt{2}/N$ described in Equation 1.
- Outputs: Three single-phase estimated phasors

C. Symmetrical Component Calculation (Figure 7)

- Inputs: Three single-phase estimated phasors
- Functions: The positive-, negative-, and zero-sequence components are estimated in the this block. The main output is the positive-sequence phasor used for the frequency estimation block. The negative- and zero-sequence components are also computed. They are useful for exploring unbalanced power system operation, especially in distribution systems.
- Outputs: Positive-, negative-, and zero-sequence phasors

D. Frequency Estimation (Figure 8)

- Inputs: Positive-sequence phasor
- Functions: The frequency is estimated using the positive-sequence phasor angle following the algorithm described in Section II-B. The first block converts the phasor from rectangular to polar coordinates and extracts the angle. This angle is sent to a buffer block where the sampled phasor measurement series is created. The data set is sent to a MATLAB function that processes the data and estimates the frequency deviation in Hz. The frequency deviation is used to estimate the complex gain P_n.
- Output: Frequency deviation

E. Table Lookup (Figure 9)

- Inputs: Positive-sequence phasors (P_PS) and frequency deviations (FD)
- Functions: The main goal of this block is the estimation of the complex gain P_n used for correct the phasor under

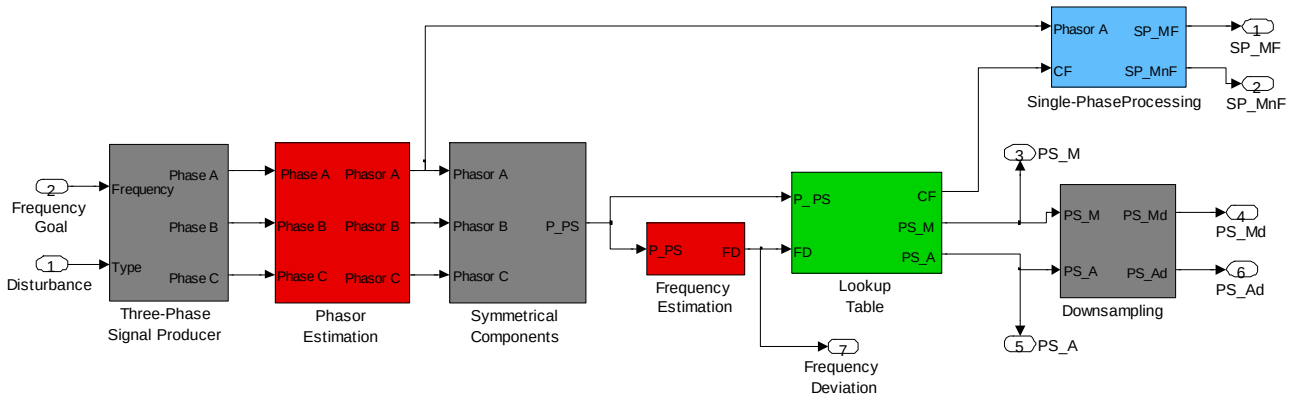

Fig. 5. Main Components

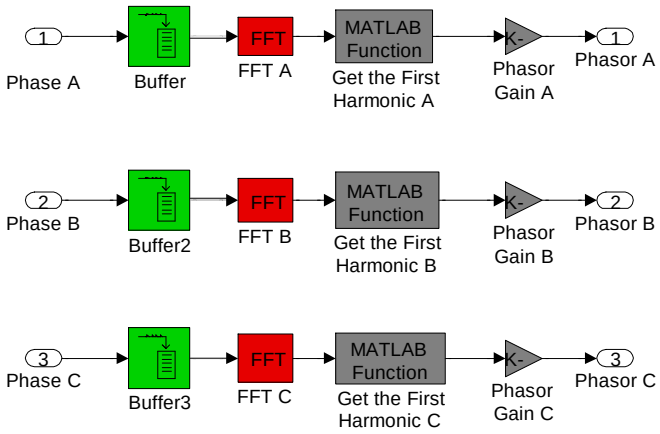

Fig. 6. Phasor Estimation Block

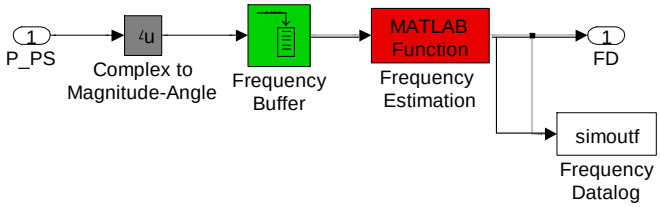

Fig. 8. Frequency Estimation Block

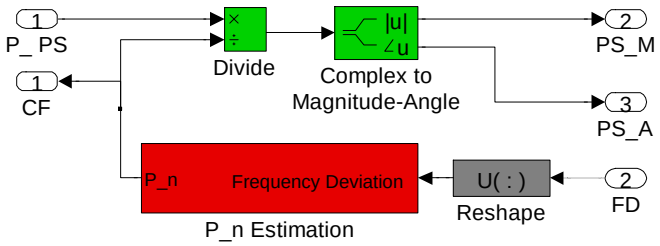

Fig. 9. Table Lookup Block

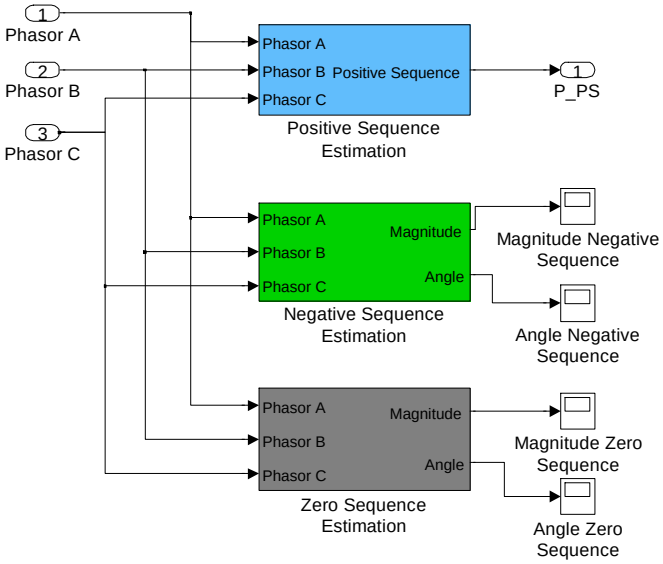

Fig. 7. Symmetrical component computation block

off-nominal frequency operation. This complex gain is estimated from frequency deviation and the window size (N) following the Equation 4. With the complex gain estimation the positive-sequence phasor is calibrated and converted to polar coordinates. The table lookup block is presented in Figure 9.

- Outputs: Calibration factors (CF), positive-sequence magnitude (PS_M), and positive-sequence angle (PS_A)

F. Downsampling

- Inputs: The magnitude (PS_M) and angle (PS_A) of positive-sequence phasors
- Functions: In this block the phasors are downsampled to generate the real PMU output. A sample is picked up every N points of a phasor, decreasing the sampling rate from $N * f_{\text{nominal}}$ to f_{nominal}.[2]
- Outputs: Down-sampled positive-sequence magnitude (PS_Md) and angle (PS_Ad) of phasors

[2]Note that some commercial PMUs computes phasors directly at the nominal sampling rate f_{nominal}.

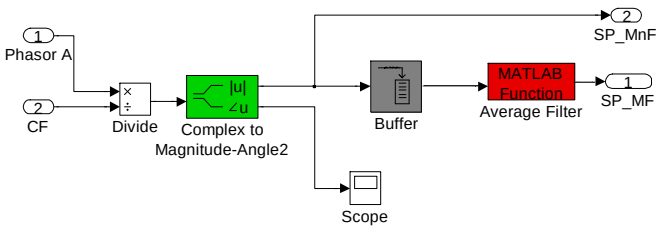

Fig. 10. Single-Phase Processing

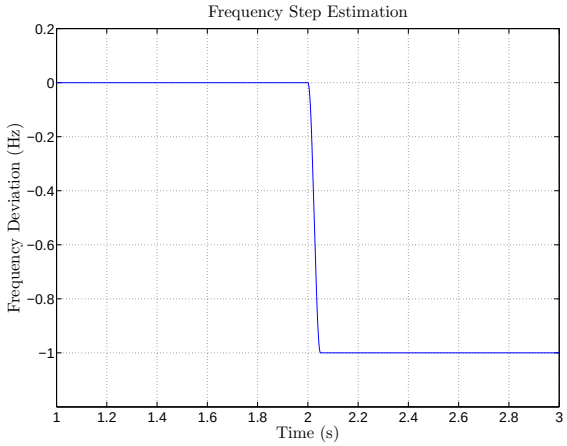

Fig. 11. Frequency Deviation Estimated

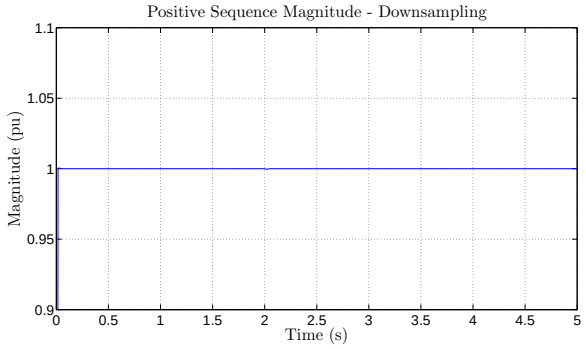

Fig. 12. Positive-Sequence Phasor Magnitude from Step and Ramp Disturbances)

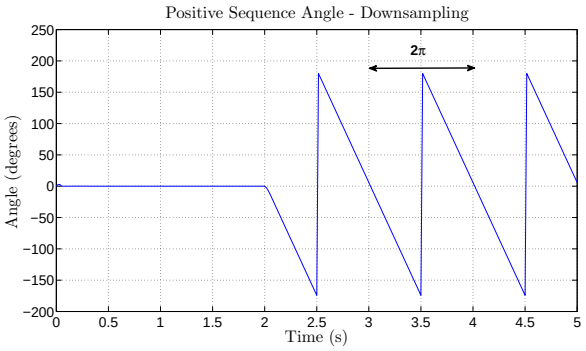

Fig. 13. Positive-Sequence Phasor Angle from Step Disturbance

G. Single-Phase Processing (Figure 10)

- Inputs: Single-phase phasors and calibration factors (CF)
- Functions: A separate block for single-phase phasor processing is necessary because of the second harmonic oscillation introduced by the complex gain Q at off-nominal frequencies. The effect of the complex gain Q is automatically compensated in the positive sequence estimation. The processing starts with the calibration regarding the effects of the complex gain P. After the phasor is converted into polar coordinates, the traditional three-point average filter is applied for second harmonic filtering. The intent is to show the second harmonic effect comparing single-phase phasor magnitude with and without filtering at off-nominal frequencies.
- Outputs: Single-phase phasor magnitude with and without filtering

IV. Examples of Educational Activities

In this section, educational components using the PMU simulator are illustrated. In the examples, the nominal system frequency is 60 Hz, for the simulated signals, a sampling rate of 32 points per cycle, that is, 1920 Hz is used.

A. Positive-Sequence Phasor Computation

1) Step Disturbance: A three-phase system is used to show the positive-sequence estimation performance. A frequency step (*Switch* 1 set on step) of one Hz (*Switch* 2 set on 59) is applied after two seconds. Figure 11 shown the frequency estimation deviation for this case.

The phasor magnitude and phase after downsampling are shown in the Figures 12 and 13, respectively. This example is suitable for understanding the angle behavior under off-nominal frequency operation. After the disturbance application, the phasor angle starts to decrease linearly following the frequency drop. A frequency deviation of 1 Hz corresponds to an angle variation of 2π/sec.

2) Ramp Disturbance: In this case, a positive 1 Hz ramp frequency disturbance is applied (Switch one in ramp position) between two and three seconds. The performance of the positive-sequence angle is shown in Figure 14.

Different from the frequency step case, the angle shows a parabolic behavior under the frequency ramp period (2-

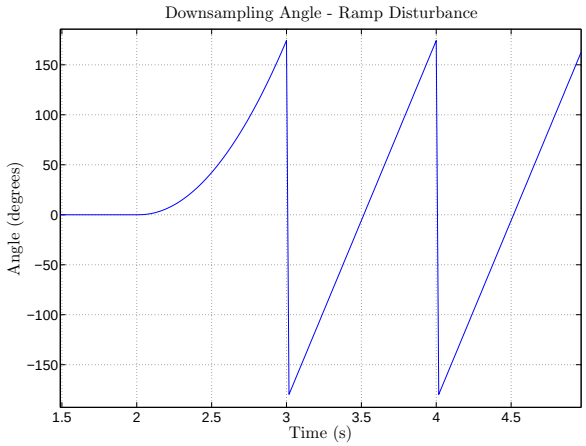

Fig. 14. Positive Sequence Angle from Ramp Disturbance

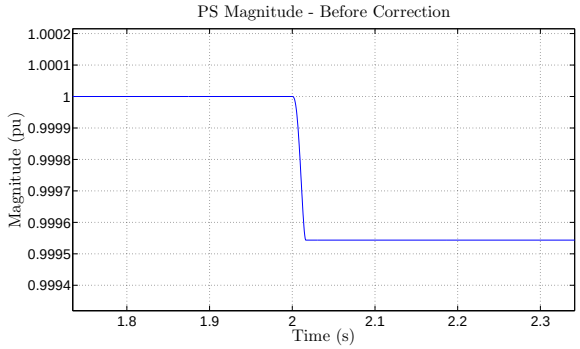

Fig. 15. Complex Gain P_n Influence from Step Disturbance

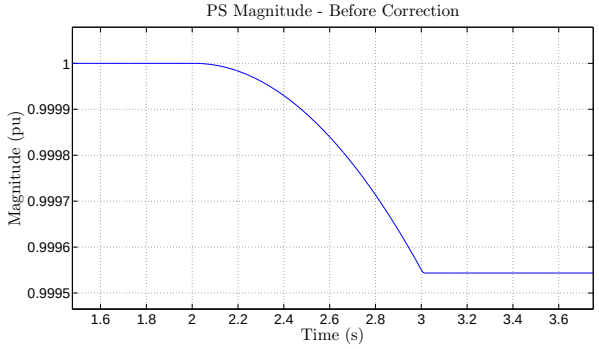

Fig. 16. Complex Gain P_n Influence from Ramp Disturbance

3 seconds). The system acceleration is positive (frequency rising) so the position (angle) is increasing.

3) Complex Gain Influence: The complex gain Q_n, a second harmonic oscillation, does not affect the positive sequence phasor performance because it is filtered by the three-phase estimation. The influence of the complex gain P_n under off-nominal frequency operation, when the calibration block is not considered, is shown in Figure 15. During the off-nominal frequency operation the leakage phenomena result in a attenuation of the magnitude of the phasor.

For the ramp disturbance, the performance of the positive-sequence phasor magnitude is shown in Figure 16.

B. Single-Phase Phasor Computation

For the step disturbance, the influence of the complex gain Q_n is clearly observed in the single-phase phasor estimation under off-nominal frequency and is shown in Figure 17. In this example the influence of the complex gain is clearly revealed in the phasor magnitude before the filtering and downsampling blocks. A second harmonic of 120 Hz shows up in the phasor magnitude without filtering (blue curve). The phasor magnitude after filtering is shown in the red curve. The single-phase phasor performance after filtering and downsampling is shown in Figure 18. A low-amplitude oscillation at 2 Hz is observed.

C. Unbalanced Operation

In this example, the phasor magnitudes are changed in the *Signal Generator* block (Figure 19) to simulate a 5% unbalanced in the three-phase signals, as shown in Figure 20. The

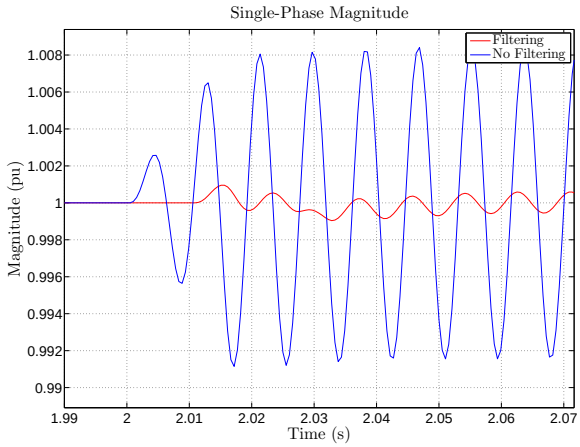

Fig. 17. Single-Phase Phasor Magnitude Estimation

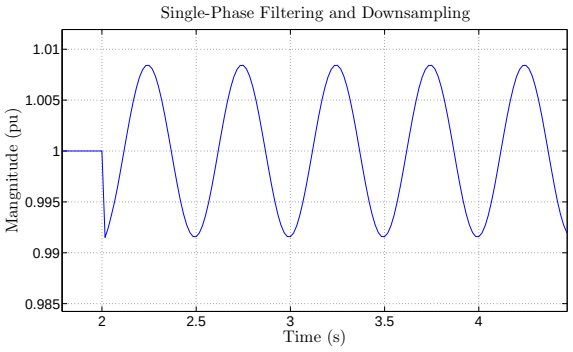

Fig. 18. Single-Phase Phasor Magnitude Estimation with Downsampling

positive- and zero-sequence phasor magnitude are shown in Figures 20 and 21, respectively. Note that the second-harmonic components will not be canceled in the positive-sequence calculation under unbalanced operation. An oscillation of 2 Hz is evident under off-nominal frequency operation.

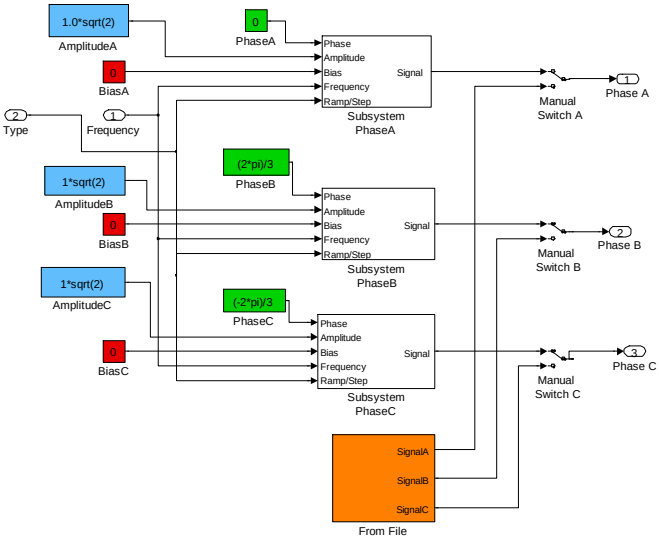

Fig. 19. Unbalanced operation setting

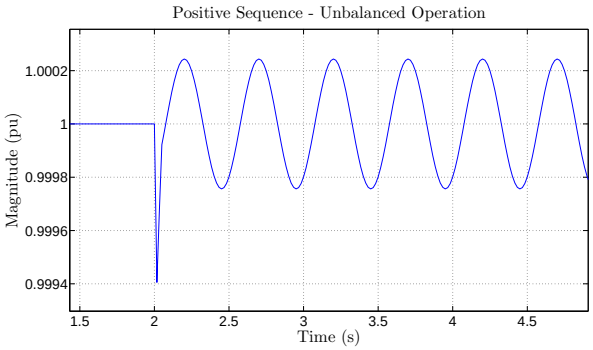

Fig. 20. Positive-sequence phasor magnitude under off-nominal and unbalanced operation

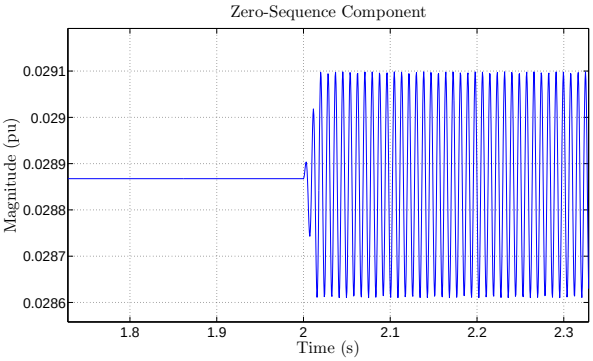

Fig. 21. Zero-sequence phasor magnitude under off-nominal and unbalanced operation

D. Real Data

Real digital data files can be also processed by the PMU Simulator. The data was recorded at 48 points per cycle, that is, a sampling rate of 2.88 kHz. The results are presented as follows.

1) Generator load rejection: A three-phase real digital data acquired during a generator load rejection test is processed by the simulator. The three-phase voltage and current data acquired during the fault are shown in Figures 22 and 23, respectively.

It should be noted that the load rejection happened around 0.35 s., the voltage wave exhibits some spikes related with the circuit breaker misoperation. In the current plots the breaker misoperation can be also observed. The frequency estimation before and after the disturbance is shown in Figure 24.

Following the load rejection, the frequency rises significantly because the generator is operating with no load. As expected there is a delay related to the actuation of the speed governor. The positive- and negative-sequence magnitude from the current phasor estimation is presented in Figures 25 and 26. The breaker is clearly observed in the increase of negative-sequence component around 0.37 s.

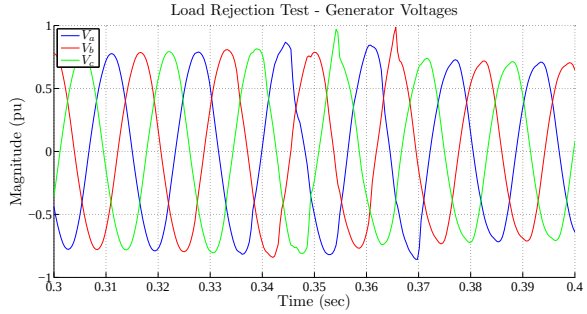

Fig. 22. Three-Phase Real Voltage Data

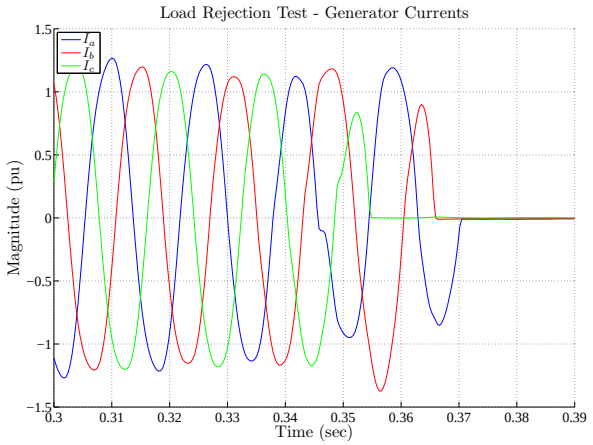

Fig. 23. Three-Phase Real Current Data

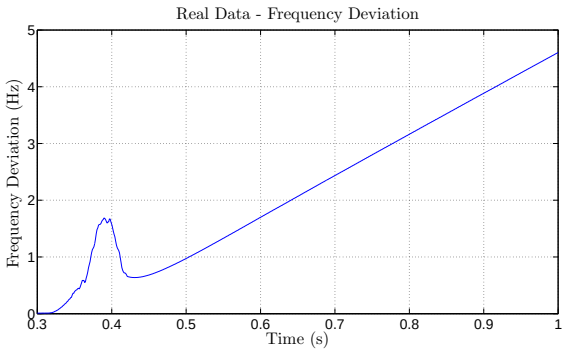

Fig. 24. Frequency Performance

V. Conclusions

In this paper a PMU Simulink simulator was presented. The aim of this software is to aid in the understanding of the behavior of algorithms internal to the PMU and to grasp key factors affecting their performance under off-nominal frequency operation. The PMU simulator is useful for academics

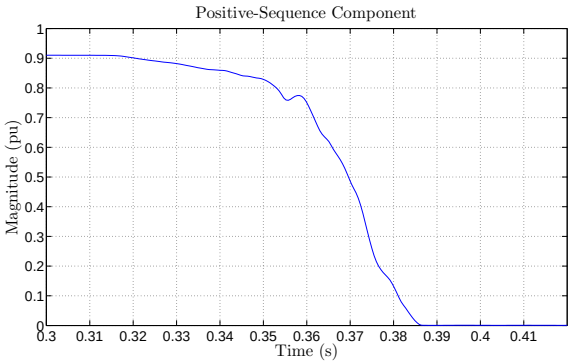

Fig. 25. Positive-Sequence Component of Current

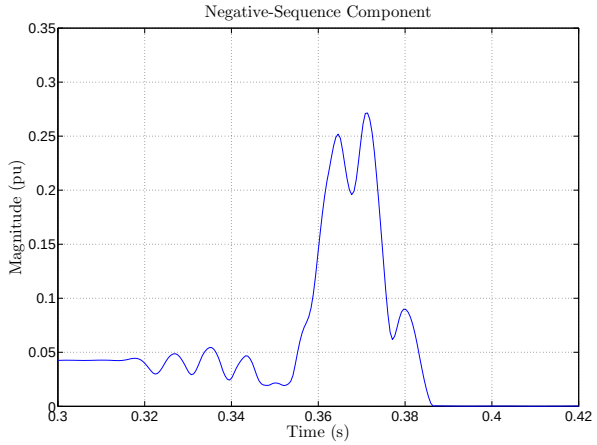

Fig. 26. Negative-Sequence Component of Current

and professionals who would like to understand the concepts involved in the phasor estimation process carried out by PMUs. The data block SIMULINK environment allows a better understanding of the algorithms and data flow involved in the phasor measurement process. This open environment also provides an easy access to the signals the user wants to observe. The data block format and the real time operation mode are improvements over a preliminary simulator discussed in [10].

ACKNOWLEDGMENT

The authors gratefully acknowledge the financial support of the Brazilian Government Research Agency (CNPq) grant 201249/2011-1 and Dr. Jay Murphy for the discussions on phasor measurement estimation. The work is also supported in part by the Engineering Research Center Program of the NSF and the DoE under Award Number EEC-1041877 and the CURENT Industry Partnership Program.

REFERENCES

[1] X. Xie, Y. Xin, J. Xiao, J. Wu, and Y. Han, "WAMS applications in Chinese power systems," *IEEE Power Energy Mag.*, vol. 4, no. 1, pp. 54–63, 2006.

[2] I. C. Decker, A. S. e Silva, M. N. Agostini, F. B. Prioste, B. T. Mayer, and D. Dotta, "Experience and applications of phasor measurements to the Brazilian interconnected power system," *European Transactions on Electrical Power*, vol. 21, no. 4, pp. 1557 – 1573, May 2011.

[3] DoE, "Smart grid investment grant program - progress report," US Department of Energy, Tech. Rep., 2012.

[4] J. Y. Yanshan Yu and B. Chen, "The smart grids in China - A review," *Energies*, vol. 5, pp. 1321–1338, 2012.

[5] M. Akke and J. S. Thorp, "Sample value adjustment improves phasor estimation at off-nominal frequencies," *IEEE Trans. on Power Delivery*, vol. 25, no. 4, pp. 2255–2263, 2010.

[6] I. C. Decker, M. N. Agostini, A. S. e Silva, and D. Dotta, "Monitoring of a large scale event in the Brazilian power system by WAMS," in *Proc. VIII iREP*, 2010, pp. 1–8.

[7] C. Ruiz, N. Orrego, and J. Gutierrez, "The Colombian 2007 black out," in *Trans. and Distr. Conf. and Exposition: Latin America, 2008 IEEE/PES*, 2008.

[8] D. Dotta, A. S. e Silva, and I. C. Decker, "Design of power system controllers by nonsmooth, nonconvex optimization," in *Proc. IEEE Power & Energy Society General Meeting PES '09*, 2009, pp. 1–7.

[9] *IEEE Std C37.118.1-2011 (Revision of IEEE Std C37.118-2005)*, IEEE Synchrophasor Measurements for Power Systems Std., 2011.

[10] D. Dotta, J. H. Chow, L. Vanfretti, M. S. Almas, and M. N. Agostini, "A MATLAB-based PMU simulator." IEEE PES General Meeting 2013, 2013.

[11] A. G. Phadke and B. Kasztenny, "Synchronized phasor and frequency measurement under transient conditions," *IEEE Trans. Power Del.*, vol. 24, no. 1, pp. 89–95, 2009.

[12] W. Premerlani, B. Kasztenny, and M. Adamiak, "Development and implementation of a synchrophasor estimator capable of measurements under dynamic conditions," *Power Delivery, IEEE Transactions on*, vol. 23, no. 1, pp. 109 –123, jan. 2008.

[13] G. C. Zweigle, L. S. Anderson, and A. Guzman-Casillas, "Tapparatus and algorithm for estimating synchronized phasors at pre-determined times referenced to an absolute time standard in an electrical system," US Patent 7 480 580, 20, 2009.

[14] D. W. P. Thomas and M. S. Woolfson, "Evaluation of frequency tracking methods," *IEEE Trans. on Power Delivery*, vol. 16, no. 3, pp. 367–371, 2001.

[15] M. M. Begovic, P. M. Djuric, S. Dunlap, and A. G. Phadke, "Frequency tracking in power networks in the presence of harmonics," *IEEE Trans. Power Del.*, vol. 8, no. 2, pp. 480–486, 1993.

[16] M. Akke, "Frequency estimation by demodulation of two complex signals," *IEEE Trans. Power Del.*, vol. 12, no. 1, pp. 157–163, 1997.

[17] D. Fan and V. Centeno, "Phasor-based synchronized frequency measurement in power systems," *IEEE Trans. Power Del.*, vol. 22, no. 4, pp. 2010–2016, 2007.

[18] ——, "Least-squares estimation in phasor-based synchronized frequency measurements," in *Proc. IEEE Power and Energy Society General Meeting - Conversion and Delivery of Electrical Energy in the 21st Century*, 2008, pp. 1–6.

[19] A. Phadke, J. Thorp, and M. Adamiak, "A new measurement technique for tracking voltage phasors, local system frequency, and rate of change of frequency," *IEEE Trans. on Power Apparatus and Systems*, vol. PAS-102, no. 5, pp. 1025 –1038, may 1983.

[20] A. G. Phadke and J. S. Thorp, *Synchronized phasor measurements and their applications*. New York: Springer, 2008.

[21] D. Dotta and J. Chow, "Second harmonic filtering in phasor measurement estimation," *Power Delivery, IEEE Transactions on*, vol. 28, no. 2, pp. 1240–1241, 2013.

Daniel Dotta received his PhD Degree in Power System Engineering in 2009, from the Federal University of Santa Catarina, Florianpolis, Brazil. He has been on the faculty at the Federal Institute of Santa Catarina since 2006. Currently he is doing his sabbatical at Renssenlaer Polytechnic Institute (RPI), Troy, NY, USA.

Joe H. Chow received his MS and PhD degrees from the University of Illinois, Urbana-Champaign. After working in the General Electric power system business in Schenectady, he joined Rensselaer Polytechnic Institute in 1987, and is a professor of Electrical, Computer, and Systems Engineering. His research interests include multivariable control, power system dynamics and control, voltage-source converter-based FACTS controllers, and synchronized phasor data applications.

David Bertagnolli is a principal engineer with ISO-New England, the Independent System Operator for the New England bulk electric power system. Mr. Bertagnolli holds a Bachelors degree in electrical engineering from the University of Illinois and a Masters degree from Columbia University. He is registered as a Professional Engineer in the State of Connecticut and a senior member of the Institute for Electrical and Electronics Engineers.